A NOVEL BACKTRACKING APPROACH FOR TWO-AXIS SOLAR PV TRACKING PLANTS

L.M. Fernández-Ahumada[1], J. Ramírez-Faz[2], R. López-Luque[3], M. Varo-Martínez[3,*], I.M. Moreno-García[4], F. Casares de la Torre[2]

[1] Computing and Numeric Analysis. University of Cordoba. Campus of Rabanales, 14071 Cordoba, Spain.

[2] Electrical Engineering. University of Cordoba. Campus of Rabanales, 14071 Cordoba, Spain.

[3] Applied Physics. University of Cordoba. Campus of Rabanales, 14071 Cordoba, Spain.

[4] Electronic and Computers Engineering. University of Cordoba. Campus of Rabanales, 14071 Cordoba, Spain.

*Corresponding Author: Phone: + 34957218602 Fax: + 34957212068 e-mail address: fa2vamam@uco.es

ABSTRACT

Solar tracking is a technique required to increase energy production in multiple photovoltaic (PV) facilities. In these plants, during low-elevation solar angle hours, shadows appear between the collectors causing a dramatic decrease in production. This paper presents a novel optimal tracking strategy to prevent the creation of these shadows. The presented method determines whether or not there is shading between collectors. Thus, when the collectors are not shaded, a tracking trajectory for maximum irradiance on the collectors is suggested. However, when the collectors are shaded, backtracking is proposed. Therefore, energy production in plants with this novel tracking method can be 1.31 % higher than that in PV installations with astronomical tracking. Moreover, this method allows the study of PV facilities for which there have been no published approaches, such as plants with non-rectangular collectors or those located on topographically heterogeneous surfaces.

KEYWORDS: PV Solar Plants, Two-axis Solar Tracker, Power Losses by Shading in PV Plants, Backtracking.

1. INTRODUCTION

Technologies based on the use of solar energy have recently received more attention, and their development aims to respond to the growing need for renewable energy. In this context, scientific advances in the field of photovoltaics (PV) are allowing this technology to become an alternative sustainable energy source [1, 2]. However, these advances are not always properly applied to PV plant design and/or operation, and, consequently, the optimal development that these advances require for PV plants has not yet been achieved.

This is evident in the case of using solar tracking to increase the ability of PV plants to harness solar resources. Solar trackers can be classified as one- or two-axis trackers. In one-axis trackers, the collector's surface rotates around a fixed axis, while the surface moves around two fixed axes in two-axis trackers, which allows the collector plane to orientate towards any direction of the celestial sphere [3]. In this research area, authors [4, 5, 6] have analysed the effects of the type of tracking on energy production at different latitudes, and their results show that, in any case, the higher the latitude, the more effective the tracking, with differences reaching 57% [7].

In solar tracking PV plants, the collector's orientation is commonly governed by equations based on the astronomical movement of the Sun, which can predict the position of the Sun in the celestial sphere with an accuracy of an order of mrad [8-10]. In this field, mathematical equations based on applying spherical trigonometry to solar movement have been developed to calculate the elevation and azimuth position for one- and two-axis trackers for each moment [7,10-14]. Recently, in contrast to this method, it is possible to deduce all of the astronomical factors governing the movement of the Sun and the orientation of solar tracking systems from the definition of 'solar vector' (unit vector along the direction towards the centre of the solar disk) and applying vector algebra [15-19].

Applying the astronomical model to solar tracking means that the angle formed between the direct solar rays and the normal angle to the collector's surface θ must be as low as possible. With astronomical tracking, the value of the direct irradiance component is maximized, which is appropriate for applications focused on this component (such as concentration technologies). However, in PV, all irradiance components (direct, diffuse, and reflected irradiance) are usable. Therefore, this type of tracking is not the most suitable. As Duffie and Beckman [11] and Mousazadeh et al. [2] noted, on cloudy days, when the solar disk is not visible and direct radiation does not reach the collectors,

collectors located on a fixed horizontal position would collect more energy than those with astronomical tracking. Despite this, no work has been conducted to determine the appropriate equations for optimising solar tracking on cloudy days. Thus, it is necessary to study the influence of diffuse and reflected components on solar tracking in greater depth to determine the equations that can allow maximum radiative capture.

Additionally, one of the most important aspects to consider in plants with astronomical solar tracking is shading between the modules, which mainly occurs during the first and last hours of the day and causes production losses, as well as the appearance of hot spots in the modules [7].

To characterise and optimise the design of tracking plants, Diaz-Dorado et al. [20-21] developed a model that considers the arrangement of the cells within the photovoltaic modules, as well as the exact position of each module within the tracking surface, to determine the shading effects for all cells in the tracker. In this model, shading is characterised following a conventional tracking strategy to achieve perpendicularity between the direct solar rays and the collector’s surface [20-21].

To estimate power losses caused by shading, Martinez-Moreno et al. [22] have proposed a predictive model that does not require any specific information regarding the connections between the cells and modules. This model has been validated by different authors [23, 24] who have developed more extensive models based on Martinez-Moreno’s model to determine the productivity of PV plants. Similarly, Perpiñan [25] developed a method for estimating and optimising energy costs based on plant design parameters, specifically the ground cover ratio (GCR, which is the ratio between the PV module area and the terrain occupied by the PV plant). For this, the method uses Gordon and Wenger’s hypothesis [26] when determining energy losses due to shading, which considers the losses proportional to the percentage of the shaded area. Navarte and Lorenzo [27] studied the productivity of a PV plant considering different types of solar tracking and three simple hypotheses for estimating losses by shading.

Panico et al. [28] proposed backtracking as an approach to minimise the effects of shading. This technique involves deviating the direction of the solar trackers from the solar position to avoid shading between the collectors when necessary. Different authors [7, 28, 29] have demonstrated the advantages of backtracking, as follows:

A. Advantages of land use: By avoiding the effects of shading, the distances between trackers can be reduced, resulting in greater GCR.

B. Operating advantages: The work conducted by Lorenzo and Navarte [7] indicates that, in all cases, energy balance is more favourable in plants with backtracking than in those allowing shading between collectors.

C. Design advantages: The absence of shading and, therefore, of hot spots, suggests lower maintenance costs.

Therefore, the reliability of plants with backtracking is greater than that in plants that allow shading [7,29]. Consequently, many technological solutions to implement backtracking are being developed [30-32].

To determine the orientation of the collectors during backtracking, different methods based on the geometric determination of shadows between polygons have been proposed [4,7,33]. However, these methods are often limited to simple geometric situations such as:

i. Exclusively rectangular collectors.

ii. Regular ground layouts where only the shading between contiguous collectors is considered.

iii. Flat topographic surfaces.

iv. Horizontal topographic surfaces.

v. Movement around the azimuthal and elevational axes without considering other combinations of axes that entail the rotation of the collector around the normal axis to the collector's surface.

Considering the aforementioned limitations, this study presents a simple and more generic backtracking method to avoid shadows and optimise solar energy collection. The method is based on the vector treatment of the geometry of the Sun-Earth position, as well as the implicit geometry of solar tracking plants. Furthermore, this method does not *a priori* assume the astronomical tracking hypothesis commonly assumed in the literature, which aims to maintain the position of the collector's surface perpendicular to the direct solar rays [15]. Thus, the proposed method allows the following, which are novelties in comparison to conventional methodologies:

1. The study of plants with non-rectangular surface collectors.
2. The analysis of facilities where collectors are not necessarily located at the regular nodes of a geometric grid.
3. The determination and comparison of the effects of different tracking modes.
4. The consideration of plants located on real topographical surfaces, and not only flat or horizontal surfaces.

5. The consideration of global irradiance on collectors, instead of being limited to direct irradiance (typical for astronomical tracking).

Therefore, the method presented here will be useful for optimising the design of new photovoltaic two-axis tracker plants, as well as for controlling the movement of current plants by improving and optimising their electrical production.

2. MATERIALS AND METHODS

2.1 Astronomical and Vector Fundamentals

To optimise the trajectory of solar trackers in PV plants, this work is based on the definition of the solar vector $\vec{s}$ in an Earth reference system, where the Ox axis is oriented to the West, the Oy axis is oriented to the South, and the Oz axis is oriented to the zenithal direction, with $\vec{i}$, $\vec{j}$, and $\vec{k}$ the respective unit vectors (Figure 1). The solar vector is given by equation (1), where δ is the solar declination [16] and *Ωt* is the hourly angle, which is defined as the product of the Earth's rotation speed (*Ω= 2π/24 rad/h)* and the time elapsed since the solar noon.

$$\vec{s} = s_x\vec{i} + s_y\vec{j} + s_z\vec{k} = \sin\Omega t\cos\delta\,\vec{i} + (\cos\Omega t\cos\delta\sin\varphi - \sin\delta\cos\varphi)\,\vec{j} + \\ + (\cos\Omega t\cos\delta\cos\varphi + \sin\delta\sin\varphi)\,\vec{k} \qquad (1)$$

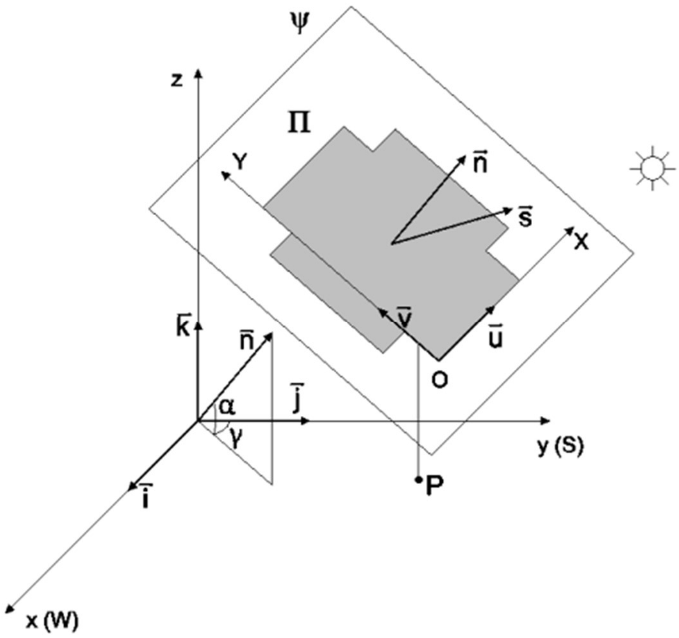

Figure 1. Representation of the collector's surface in the Earth reference system

Figure 1 also shows the polygon *Π*, which represents the perimeter of the collector's surface, and the vector normal to that surface, $\vec{n}$. The components of the vector $\vec{n}$ in the Earth reference system, depending on the azimuth *(γ)* and elevation *(α)* angles of the collectors, are given by equation (2).

$$\vec{n}= \cos\alpha \cdot \sin\gamma\vec{i} + \cos\alpha \cdot \cos\gamma\vec{j}+ \sin\alpha\vec{k} \qquad (2)$$

Additionally, the projection plane is considered as the plane that contains the collector's surface. A flat coordinate system associated with this plane is defined (OXY) with unit vectors $\vec{u}$ and $\vec{v}$. During tracking, the system will move while rigidly attached to the collector polygon. As a result, the mathematical expressions for $\vec{u}$ and $\vec{v}$ will depend on the collector's orientation at every moment, given by α and γ, and be conditioned by the type of tracking. Equations (3)-(16) present the expressions for the most frequent tracking typologies (shown in Figure 2).

- Azimuth-elevation tracking (A-E)

$$\vec{u}=- \cos\gamma\vec{i}+ \sin\gamma\vec{j} \qquad (3)$$

$$\vec{v}= \sin\alpha \cdot \cos\gamma\vec{i}- \sin\alpha \cdot \cos\gamma\vec{j}+ \cos\alpha\vec{k} \qquad (4)$$

- Equatorial tracking (EQ)

$$\vec{u}=-\cos\theta_1\vec{i}+ \sin\theta_1 \cdot \cos\varphi\vec{j}+ \sin\theta_1 \cdot\sin\varphi\vec{k} \qquad (5)$$

$$\vec{v}=-\sin\theta_2\cdot\sin\theta_1\vec{i}-(\cos\theta_1\cdot \sin\theta_2\cdot\cos\varphi+ \cos\theta_2\cdot\sin\varphi)\vec{j} -(\cos\theta_1\cdot \sin\theta_2\cdot\sin\varphi- \cos\theta_2\cdot\sin\theta_1)\vec{k} \qquad (6)$$

where

$$\theta_1= \tan^{-1}\left(\frac{\cos\alpha\cdot\sin\gamma}{\cos\alpha\cdot\cos\gamma\cdot\cos\varphi-\sin\alpha\cdot\sin\varphi}\right) \qquad (7)$$

$$\theta_2= \sin^{-1}(\cos\alpha\cdot \cos\gamma \cdot\sin\varphi+ \sin\alpha \cdot\cos\varphi) \qquad (8)$$

- Elevation-Rolling tracking (E-R)

$$\vec{u}=- \cos\theta_2\vec{i}+ \sin\theta_1\cdot\sin\theta_2\vec{j}+\cos\theta_1\cdot\sin\theta_2\vec{k} \qquad (9)$$

$$\vec{v}=- \cos\theta_1\vec{j}+ \sin\theta_1\vec{k} \qquad (10)$$

where

$$\theta_1=\tan^{-1}(\cos\gamma\cdot\mathrm{cotan}\,\alpha) \qquad (11)$$

$$\theta_2=\sin^{-1}(\cos\alpha\cdot\sin\gamma) \qquad (12)$$

- Rolling-Elevation tracking (R-E)

$$\vec{u}=-\cos\theta_1\vec{i}+\sin\theta_1\vec{k} \qquad (13)$$

$$\vec{v}=\sin\theta_1\cdot\cos\theta_2\vec{i}+\sin\theta_2\vec{j}+\cos\theta_1\cdot\cos\theta_2\vec{k} \qquad (14)$$

where

$$\theta_1 = tan^{-1}(sin\gamma \cdot cos\alpha) \quad (15)$$

$$\theta_2 = cos^{-1}(cos\gamma \cdot cos\alpha) \quad (16)$$

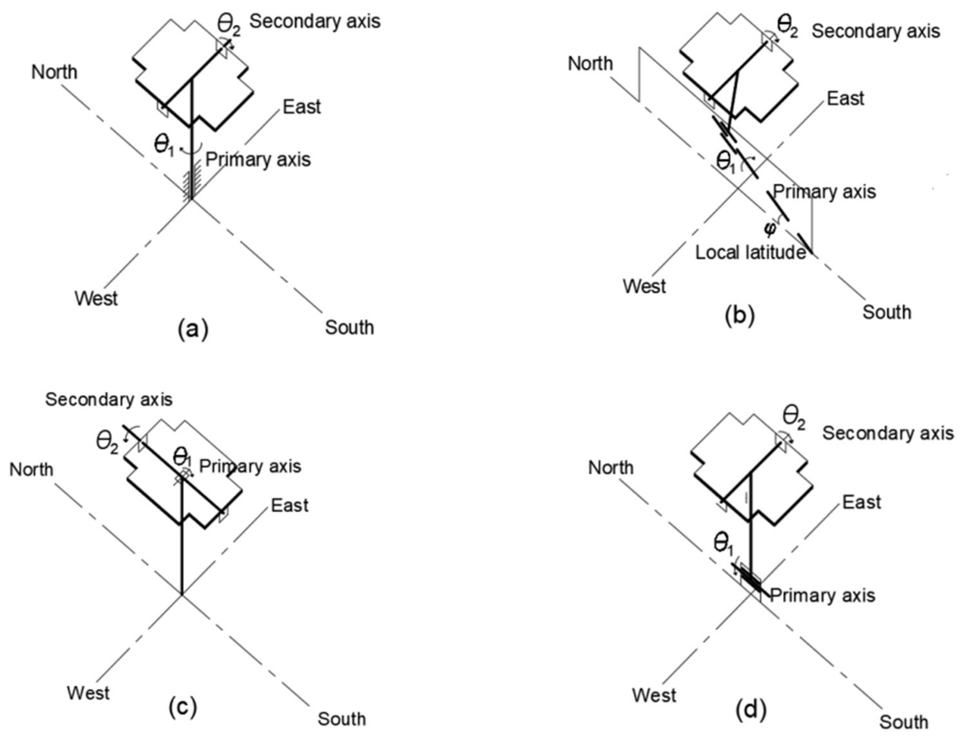

Figure 2. Common tracking strategies: a) Azimuth-elevation tracking (A-E), b) Equatorial tracking (EQ), c) Elevation-Rolling tracking (E-R), and d) Rolling-Elevation tracking (R-E)

2.2 Geometrical Methodology

Based on the geometric fundamentals defined in the previous section, this work studies shadows to dichotomously determine whether there is an intersection between the PV collectors at a specific time, rather than to quantify the shape and size of the shaded polygons. Therefore, by calculating the irradiance received by the collector's surfaces for a given hour at different positions when there is no shading, the maximum irradiance position can be elucidated. Moreover, by conducting this study over a certain period, it is possible to define the trajectory of the collectors that optimises energy capture by a PV plant for each day of the year.

In this study, it is considered that all collectors have the same geometric shape and move in the same manner. Considering this, it can be stated that the planes that contain the collector surfaces are always parallel. Therefore, regardless of the solar position with respect to the collectors, the solar projection Π'_i of any collector Π_i on plane Ψ

containing the reference tracker Π_0 will produce a polygon with the same shape and dimensions as the collector polygon i (Figure 3). From this projection, it can be concluded that Π_i shades Π_0 if polygons Π_0 and Π'_i intersect.

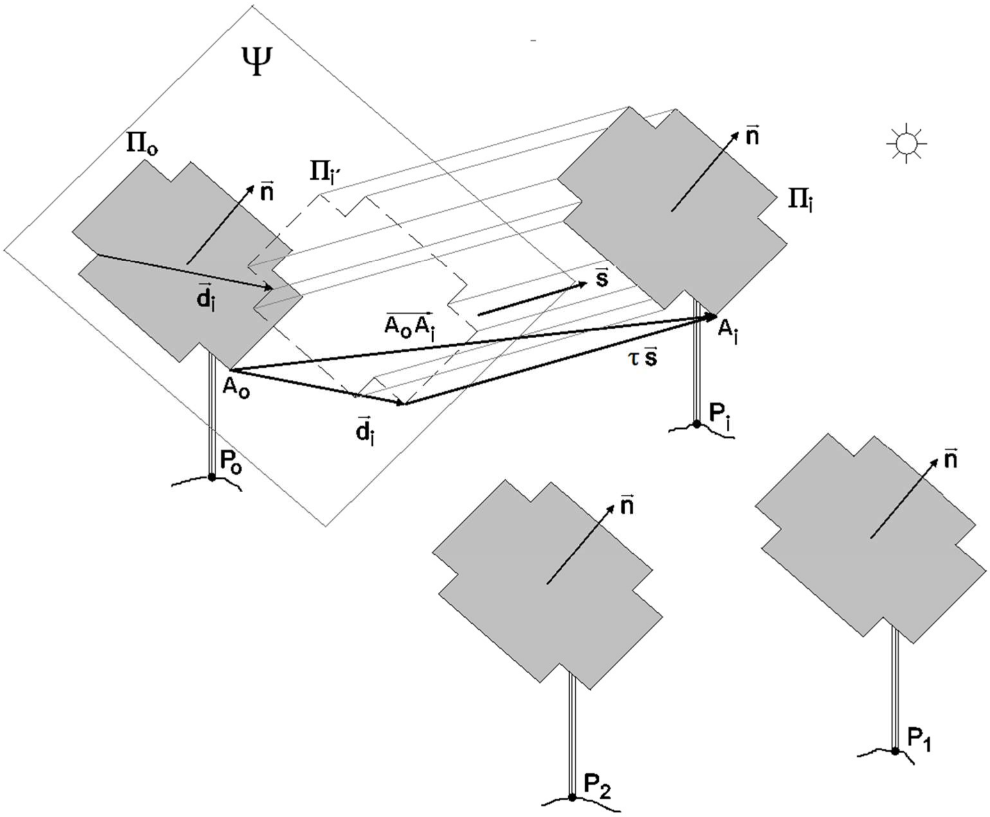

Figure 3. Geometry of the set of trackers

As all collectors are considered equal and the perimeters of the projected collectors in the solar direction maintain their geometry, polygon Π'_i could be considered as a translation of the reference collector Π_0 contained on plane Ψ, with $\vec{d_i}$ as the translation vector. Similarly, as the collectors remain parallel, the distance between any two equivalent points (A_i and A_0) of collectors Π_i and Π_0 is constant. That is, $\overrightarrow{A_0A_i}=\overrightarrow{P_oP_i}$. Consequently, to determine $\vec{d_i}$, the parallelogram rule is applied to the vectors involved in the described geometric problem (Figure 3), which produces equation (17).

$$\overrightarrow{P_oP_i}=\overrightarrow{a_0a_i}=\overrightarrow{d_i}+\tau\cdot\vec{s} \qquad (17)$$

Furthermore, to determine τ, the scalar product between equation (17) and the vector normal to plane Ψ, $\vec{n}$, is calculated, which produces equation (18), where $\vec{n}\cdot\overrightarrow{d_i}$ is zero as both vectors are perpendicular.

$$\vec{n}\cdot\overrightarrow{P_oP_i}=\vec{n}\cdot\vec{di}+\vec{n}\cdot\tau\cdot\vec{s} \qquad (18)$$

Consequently, scalar τ is given by equation (19).

$$\tau=\frac{\overrightarrow{P_oP_i}\cdot\vec{n}}{\vec{s}\cdot\vec{n}} \qquad (19)$$

Substituting (19) into (17), the translation vector of projection Π'_i with respect to reference collector Π_0 on plane Ψ, $\vec{d_i}$, can be obtained (Equation 20).

$$\vec{di}=\overrightarrow{P_oP_i}-\frac{\overrightarrow{P_oP_i}\cdot\vec{n}}{\vec{s}\cdot\vec{n}}\,\vec{s} \qquad (20)$$

Thus, expression (20) allows the components of $\vec{d_i}$ in Earth reference system Oxyz to be calculated. However, as $\vec{d_i}$ belongs to the OXY plane, the Cartesian components in the collector plane can be determined by equations (21) and (22).

$$d_X=\vec{d}\cdot\vec{u} \qquad (21)$$

$$d_Y=\vec{d}\cdot\vec{v} \qquad (22)$$

Once the projections have been obtained, a test based on Minkowski algebra [17-19] is conducted to determine whether the polygons intersect and, therefore, whether there would be shading. For this, all the feasible polygons on Ψ resulting from moving Π_0 are drawn so that any point on its perimeter matches the origin of the 0XY reference system associated with plane Ψ (Figure 4). Polygon Σ is defined as the envelope of this family of polygons. Therefore, it is possible to affirm that Π_0 and Π'_i intersect if the representation of the corresponding $\vec{d_i}$, vector moved to the origin of the 0XY reference system, is fully included in Σ (Figure 4).

To ensure that reference collector Π_0 is not shaded at a given time, it is necessary to check that it is not shaded by any other collector in the PV plant. Given that envelope Σ is the same for any pair of collectors as they all exhibit the same geometry and remain parallel, it would be sufficient to determine whether the $\vec{d_i}$ vectors (for i=1, N-1, with N being the number of PV panels in the plant) linked to each pair of collector surfaces, Π_0-Π_i, are included in envelope Σ for cases that meet the following conditions:

I. Collector Π_i is visible from the reference collector Π_0: $\overrightarrow{P_oP_i}\cdot\vec{n}>0$.
II. The sun does not irradiate the rear side of the collectors: $\vec{s}\cdot\vec{n}>0$.
III. It is a specific moment of the solar day: $\vec{s}\cdot\vec{k}>0$.

Under these conditions, a single $\vec{d_i}$ included in the Σ envelope will indicate that the studied collector is shaded.

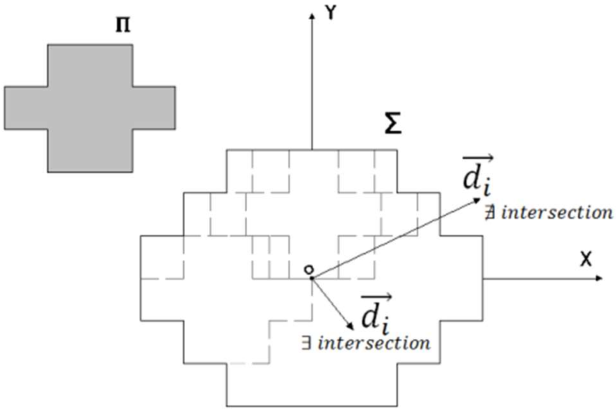

Figure 4. Obtaining enveloping polygon Σ from Π

2.3 Optimisation of the Collector Position under the no Shading Hypothesis

According to the described method, for each moment in time, whether the reference collector is shaded or not for different collector orientations (given by its azimuth, γ, and elevation, α) can be analysed. Based on this analysis, for any specific moment in time, it is also possible to represent the delimitation of the two regions in a cylindrical chart (γ, α): one corresponding to shaded collectors and another corresponding to non-shaded collectors. In addition, as will be demonstrated in the application, the irradiance received by the collectors at each orientation can be also represented on the same chart using irradiance isovalue curves. From these two delimited areas and using the irradiance isovalue curves, the point with maximum irradiance for each moment in time, and, consequently, the optimum orientation of the solar trackers, can be selected. Repeating this process for different moments in time the same day can allow the optimal tracking trajectory (with maximum irradiance and without shading) to be defined.

3. RESULTS AND DISCUSSION

Once the proposed methodology has been described, the optimal trajectories for tracking and backtracking at the "El Molino" PV solar plant located in Cordoba, Spain, are obtained (latitude=37.75492°N; longitude=5.04548°W). This plant is an Azimuth Elevation tracker plant arranged in a rectangular grid with an east-west distance (d_{EW}) of 20 m and north-south distance (d_{NS}) of 14 m (Figure 5).

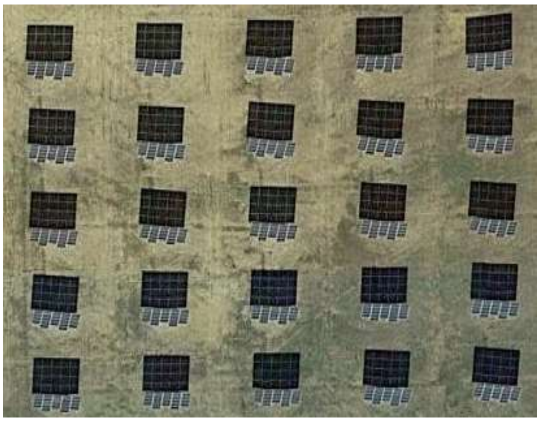

Figure 5. Application example: Spatial distribution of the collectors of the El Molino PV plant (Cordoba, Spain).

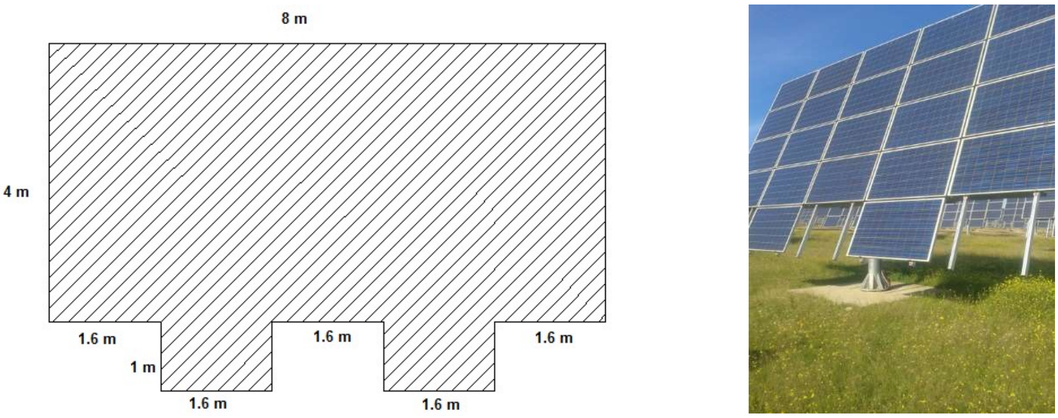

(a) (b)

Figure 6. Application example: Shape and dimensions of the photovoltaic collectors in the El Molino PV plant (Cordoba, Spain).

Based on the geometry of the collectors (Figures 6a and 6b), Figure 7 shows the envelope Σ for the collectors' surface. In practice, the polygons constituting the collectors (Figure 6a) only have right angles. Therefore, the surrounding polygon Σ has only right angles (Figure 7), simplifying the test to determine whether the $\overrightarrow{d_i}$ vectors are included in Σ. Therefore, in this example, each $\overrightarrow{d_i}$ is included in the Σ envelope if condition (23) or (24) is verified.

$$|d_{iX}|<8\ m \text{ and } |d_{iY}|<4\ m \qquad (23)$$

$$|d_{iX}|<6.4\ m \text{ and } |d_{iY}|<5\ m \qquad (24)$$

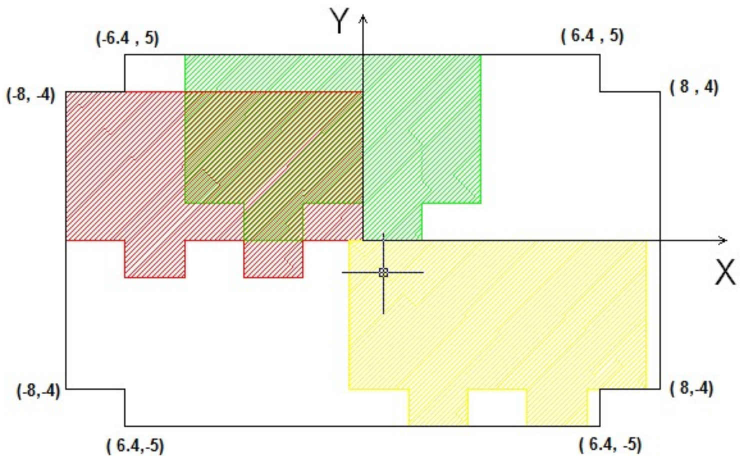

Figure 7. Application example: Shape and dimensions of polygon Σ enveloping the set of polygons generated by sliding Π_0 onto the origin of the coordinates (values in metres).

The analysis method proposed here was applied every five minutes for one astronomical year. As this methodology involves a dichotomous test to establish whether or not there is shading at a specific collector orientation defined by its azimuth *(γ)* and elevation *(α)*, a binary search for the elevation limit between the shaded and non-shaded areas has been programmed for fixed azimuth values. It has been verified that eight iterations are sufficient for estimating this limit with an error below 0.3 deg.

For Julian Day 349 at 8:20 (true solar time; TST), Figure 8 shows a cylindrical chart representing the boundary between the shaded (grey region, corresponding to the cases for which at least one $\vec{d_i}$ is included in Σ) and not-shaded (blue region, corresponding to the cases for which all vectors $\vec{d_i}$ are not included in Σ) areas. Moreover, the irradiance isolines were included in the non-shaded area. As the proposed methodology only considers the collector positions at which there would be no shading, a single irradiance model is assumed. Therefore, Liu-Jordan's equation [34] (Equation 25) was considered as it was used by Fernandez-Ahumada et al. [15], where I_B and I_D are direct and diffuse irradiances, respectively, and ρ is the albedo. In this study, $\rho=0.2$ is considered following [34]. Therefore, it is possible to determine the solar irradiance captured by the collectors for each orientation without shading using equation (25).

$$I=\frac{\vec{s}\cdot\vec{n}}{\vec{s}\cdot\vec{k}}I_B+\frac{1+\vec{k}\cdot\vec{n}}{2}I_D+\rho\frac{1-\vec{k}\cdot\vec{n}}{2}(I_B+I_D) \qquad (25)$$

Similarly, Figure 8 presents the collector orientation for three different tracking strategies:

a. Astronomical tracking with no shading (ATNS, represented by a green circle): tracking governed by an astronomic equation for an ideal PV plant where the distances between the collectors are sufficiently large to avoid shading.
b. Maximum irradiance tracking with no shading (MITNS, represented by a red circle): the optimal tracking strategy proposed by Fernandez-Ahumada et al. [15], which seeks maximum irradiance levels on an ideal isolated collector that is not affected by shadows from adjoining collectors.
c. Maximum irradiance backtracking (MIBT, represented by a blue cross): tracking strategy proposed in this study, which seeks maximum irradiance levels while avoiding shading between the collectors by backtracking when necessary.

Therefore, for this day and time, this novel backtracking approach proposes that the tracker should point towards the maximum irradiance direction within the non-shaded region (blue cross in Figure 8). Figure 8 also shows that the orientations corresponding to ATNS and MITNS are within the region where there are shadows between the collectors and, consequently, the irradiance captured by the PV modules is reduced. However, it should be noted that, in this case, the minimum and maximum limits of the azimuth or elevation are not considered. Consequently, if these constructive limits exist, they should also be represented as additional restrictions in the cylindrical charts.

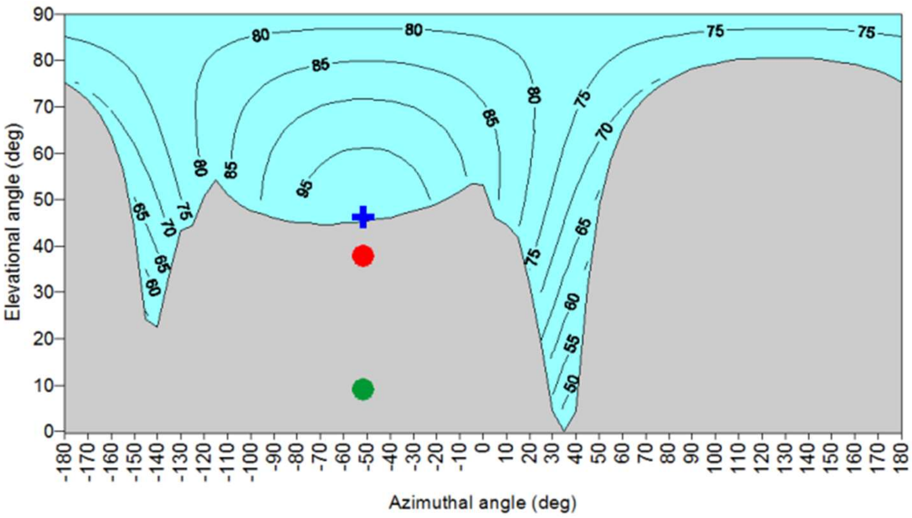

Figure 8. Application example: Splitting of the spatial directions and selection of the angles (γ, α) that optimise irradiance (W/m^2) for the reference collector in the El Molino PV plant (Cordoba, Spain) on Julian day 349 at 8:20 TST.

Moreover, based on the method outlined above, the path to be tracked by the collector for the day of study can be proposed. Therefore, Figure 9 shows the trajectories corresponding to the three different analysed tracking strategies: ATNS (green line), MITNS (red line), and MIBT (blue line). As shown, the proposed MIBT trajectory (blue curve) exhibits sections where it does not coincide with the MITNS trajectory (red curve) corresponding to the maximum solar irradiance collection under an ideal situation with no shading. For these periods, backtracking is proposed as the movement that optimises energy collection by the plant, as it considers the real shadows between the collectors, which reduce the levels of irradiance from their optimal values considered by MITNS.

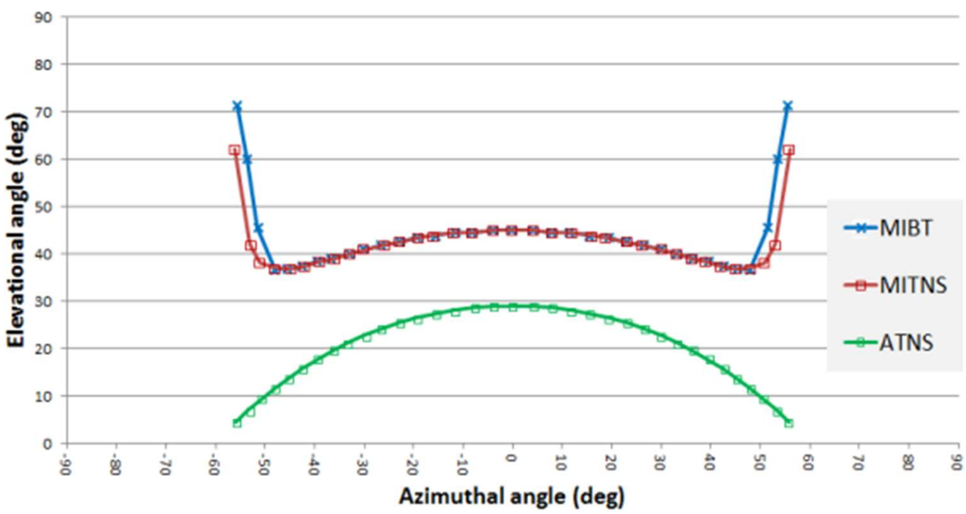

Figure 9. Application example: Potential collector pointing trajectories of the PV plant "El Molino" (Cordoba, Spain) on the Julian day=349

Finally, the daily radiation was determined for each approach to compare energy production under the three potential strategies (ATNS, MITNS, and MIBT). The values for the three cases were obtained by integrating equation (25) on representative days. Therefore, although the three tracking strategies imply no shading between collectors, in contrast to MIBT, ATNS and MITNS are only valid for isolated trackers and not for plants with many PV modules. Accordingly, the simulated energy production of these two ideal tracking strategies can be considered as maximum potential values and should be used as a reference to evaluate the improvements made by the proposed tracking method.

Table 1. Comparative analysis of the energy production levels of PV solar plants with different tracking strategies.

Month	MIBT (kWh/kWp)	MITNS (kWh/kWp)	ATNS (kWh/kWp)	Decrease in MIBT vs. MITNS (%)	Increase in MIBT vs. ATNS (%)
January	82.4	84.2	83.7	2.16	-1.51
February	114.7	116.0	114.0	1.09	0.59
March	144.3	146.3	144.4	1.36	-0.11
April	160.8	163.0	161.4	1.35	-0.39
May	177.1	179.6	178.4	1.41	-0.76
June	250.5	251.1	244.5	0.24	2.44
July	291.0	291.3	280.7	0.08	3.68
August	269.3	269.6	259.0	0.09	4.01
September	197.7	198.4	192.1	0.34	2.93
October	125.4	127.3	125.9	1.49	-0.35
November	86.6	88.5	88.0	2.11	-1.52
December	65.0	67.4	67.4	3.54	-3.49
Year	**1965.0**	**1982.7**	**1939.5**	**0.89**	**1.31**

Table 1 shows the simulated energy production (kWh) values for each month against the peak power (kWp) of the collectors. In line with Fernandez-Ahumada's results [15], energy production under MITNS is higher than that under ATNS. Similarly, it has been verified that, for several months, energy production by solar plants under MIBT reaches values between the optimal values of MITNS and ATNS. Production by MIBT solar plants is 0.89% lower than that by MINTS plants, but 1.31% higher than that by ATNS plants.

The proposed method improves the results obtained by Navarte and Lorenzo [27] in their characterisation of the energy losses due to shading in plants with different astronomical tracking typologies (one and two-axis). They demonstrated that, in all cases, energy production losses increase with GCR. Therefore, in comparison to the ideal astronomical tracking, they estimated that the uncertainty of energy production is within 2% for GCR=0.09. These results are similar to those published by Panico [28], even though this study is restricted to one-axis trackers. Specifically, Panico found that the losses due to shading in installations with GCR=0.09 compared to astronomical tracking are 2.5% [28]. These values are also within the intervals proposed by Gordon and Wenger [26], who demonstrated that energy losses by shading in plants with GCR=0.09 depend on the collectors' geometry and spatial layout.

Consequently, all published studies indicate that shading causes energy losses in comparison to energy generation under ideal astronomical tracking. Therefore, this study shows that solar energy collection by plants with the proposed tracking strategy, MIBT, is better than that by plants with astronomical tracking and only 0.98% lower than that by plants with the ideal MITNS tracking. However, owing to the scarcity of publications in this area, the authors of this paper consider that it is necessary to continue studying the influence of design parameters on energy collection by plants with MIBT, as well as to implement this novel tracking strategy in actual PV installations to evaluate its development.

4. CONCLUSIONS

In this study, a new methodology for defining the optimal tracking strategy without shading of sets of two-axis motion PV tracker collectors is proposed. In contrast to astronomical tracking, the proposed method indicates that collectors do not have to be constantly perpendicular to the direct solar rays, as it considers the diffuse and reflected irradiance, as well as the direct irradiance, reaching PV collectors. Therefore, when collectors are not shaded, a tracking trajectory seeking maximum irradiance on the collectors is suggested. However, when the collectors are shaded, backtracking is proposed. Therefore, based on the concepts of solar vectors and vector algebra, this method analyses shading between the collectors. However, the proposed technique is not based on the calculation of the area of polygon intersections; rather, it is based on whether or not such intersections are present. Consequently, in contrast with other tracking strategies found in previous studies, this novel method is based on algorithms that are significantly more simple and fast. Thus, owing to its novelties and advantages, this method is easier to be used to simulate energy production with different radiative models and is applicable to situations for which no published generic methods can be found, such as PV plants:

i. with non-rectangular surface collectors
ii. with collectors that are not located on the regular nodes of a geometric mesh
iii. with different tracking modes
iv. with trackers located on real topographical surfaces

The energy production by PV plants with this new tracking strategy, called MIBT, has been analysed and compared to two ideal tracking strategies:

1) ATNS: Astronomical tracking in an ideal PV plant where the distances between the collectors are large enough to avoid shading.
2) MITNS: optimal tracking that seeks the maximum irradiance levels on an ideal isolated collector not affected by potential shadows from adjoining collectors [15].

The results show that MIBT improves the energy collection by 1.31% in comparison to ATNS, and the energy collection is only 0.89% lower than that by MITNS plants. Therefore, considering these results and the advantages of this method, the authors consider that this method will not only be useful for designing new facilities, but could also help to improve the productivity and management of many PV plants by redefining tracking strategies.

ACKNOWLEDGEMENTS

This research is partially supported by the CLARA Project, which has received funding from the European Union's Horizon 2020 research and innovation programme under Grant Agreement No 730482. The authors thank Magtel Operaciones SL for their collaboration in this research.

REFERENCES

[1] V. Salas, E. Olias, Overview of the photovoltaic technology status and perspective in Spain, Renew. Sustain. Energy Rev. 13 (2009) 1049–1057. doi:10.1016/j.rser.2008.03.011.

[2] H. Mousazadeh, A. Keyhani, A. Javadi, H. Mobli, K. Abrinia, A. Sharifi, A review of principle and sun-tracking methods for maximizing solar systems output, Renew. Sustain. Energy Rev. 13 (2009) 1800–1818. doi:10.1016/j.rser.2009.01.022.

[3] C.-Y. Lee, P.-C. Chou, C.-M. Chiang, C.-F. Lin, Sun Tracking Systems: A Review., Sensors (14248220). 9 (2009) 3875–3890. doi:10.3390/s90503875.

[4] E. Lorenzo, M. Pérez, A. Ezpeleta, J. Acedo, Design of tracking photovoltaic systems with a single vertical axis, Prog. Photovoltaics Res. Appl. 10 (2002) 533–543. doi:10.1002/pip.442.

[5] O. Perpiñan, E. Lorenzo, M.A. Castro, R. Eyras, Energy payback time of grid connected PV systems: Comparison between tracking and fixed systems, Prog. Photovoltaics Res. Appl. 17 (2009) 137–147. doi:10.1002/pip.871.

[6] T. Huld, M. Suri, E.D. Dunlop, Comparison of potential solar electricity output from fixed-inclined and two-axis tracking photovoltaic modules in Europe, Prog. Photovoltaics Res. Appl. 16 (2008) 47–59. doi:10.1002/pip.773.

[7] E. Lorenzo, L. Narvarte, J. Muñoz, Tracking and back-tracking, 2011.

[8] M. Blanco-Muriel, D.C. Alarcón-Padilla, T. López-Moratalla, M. Lara-Coira, Computing the solar vector, Sol. Energy. 70 (2001) 431–441. doi:10.1016/S0038-092X(00)00156-0.

[9] I. Reda, A. Andreas, Solar position algorithm for solar radiation applications, Sol. Energy. 76 (2004) 577–589. doi:10.1016/j.solener.2003.12.003.

[10] J.E. Braun, J.C. Mitchell, Solar geometry for fixed and tracking surfaces, Sol. Energy. 31 (1983) 439–444. doi:10.1016/0038-092X(83)90046-4.

[11] J.A. Duffie, W.A. Beckman, Solar Engineering of Thermal Processes: Fourth Edition, 2013. doi:10.1002/9781118671603.

[12] D. Riley, C. Hansen, Sun-Relative Pointing for Dual-Axis Solar Trackers Employing Azimuth and Elevation Rotations, J. Sol. Energy Eng. 137 (2014) 031008. doi:10.1115/1.4029379.

[13] P.G. Jolly, Derivation of solar angles using vector algebra, Sol. Energy. 37 (1986) 429–430.

[14] Í. Rapp-Arrarás, J.M. Domingo-Santos, Algorithm for the calculation of the horizontal coordinates of the Sun via spatial rotation matrices, Renew. Energy. 34 (2009) 876–882. doi:10.1016/j.renene.2008.06.005.

[15] L.M. Fernández-Ahumada, F.J. Casares, J. Ramírez-Faz, R. López-Luque, Mathematical study of the movement of solar tracking systems based on rational models, Sol. Energy. 150 (2017) 20–29. doi:10.1016/j.solener.2017.04.006.

[16] E.G. Evseev, A.I. Kudish, The assessment of different models to predict the global solar radiation on a surface tilted to the south, Sol. Energy. 83 (2009) 377–388. doi:10.1016/j.solener.2008.08.010.

[17] B. Chazelle, The polygon containment problem, Adv. Comput. Res. 1 (1983) 1–33.

[18] T. Lozano-Perez, Spatial Planning: A Configuration Space Approach, (1980).

[19] F. Avnaim, J.-D. Boissonnat, Polygon placement under translation and rotation, RAIRO - Theor. Informatics Appl. 23 (1989) 5–28. doi:10.1051/ita/1989230100051.

[20] E. Díaz-Dorado, J. Cidrás, C. Carrillo, A method to estimate the energy production of photovoltaic trackers under shading conditions, Energy Convers. Manag. 150 (2017) 433–450. doi:10.1016/J.ENCONMAN.2017.08.022.

[21] E. Díaz-Dorado, J. Cidrás, C. Carrillo, Discrete I–V model for partially shaded PV-arrays, Sol. Energy. 103 (2014) 96–107. doi:10.1016/J.SOLENER.2014.01.037.

[22] F. Martínez-Moreno, J. Muñoz, E. Lorenzo, Experimental model to estimate shading losses on PV arrays, Sol. Energy Mater. Sol. Cells. 94 (2010) 2298–2303. doi:10.1016/J.SOLMAT.2010.07.029.

[23] T.O. Fartaria, M.C. Pereira, Simulation and computation of shadow losses of direct normal, diffuse solar radiation and albedo in a photovoltaic field with multiple 2-axis trackers using ray tracing methods, Sol. Energy. 91 (2013) 93–101. doi:10.1016/J.SOLENER.2013.02.008.

[24] Y. Hu, Y. Yao, A methodology for calculating photovoltaic field output and effect of solar tracking strategy, Energy Convers. Manag. 126 (2016) 278–289. doi:10.1016/J.ENCONMAN.2016.08.007.

[25] O. Perpiñán, Cost of energy and mutual shadows in a two-axis tracking PV system, Renew. Energy. 43 (2012) 331–342. doi:10.1016/J.RENENE.2011.12.001.

[26] J.M. Gordon, H.J. Wenger, Central-station solar photovoltaic systems: Field layout, tracker, and array geometry sensitivity studies, Sol. Energy. 46 (1991) 211–217. doi:10.1016/0038-092X(91)90065-5.

[27] L. Narvarte, E. Lorenzo, Tracking and ground cover ratio, Prog. Photovoltaics Res. Appl. 16 (2008) 703–714. doi:10.1002/pip.847.

[28] D. Panico, P. Garvison, H. Wenger, D. Shugar, Backtracking: a novel strategy for tracking PV systems, in: Conf. Rec. Twenty-Second IEEE Photovolt. Spec. Conf. - 1991, IEEE, n.d.: pp. 668–673. doi:10.1109/PVSC.1991.169294.

[29] M.C.-R.M. Pedro, Modelling of shading effects in photovoltaic optimization, (2016).

[30] Control Seguimiento Solar, Sun tracker control, solar nachführung - Suntrack, (n.d.).

[31] Solar production machines - Machinery and Plant Construction - Siemens Global Website, (n.d.).

[32] Lauritzen Solutions, (n.d.).

[33] D. Schneider, Control Algorithms for Large-scale Single-axis Photovoltaic Trackers, Acta Polytech. 52 (2012). doi:10.14311/1648.

[34] B.Y.H. Liu, R.C. Jordan, A Rational Procedure for Predicting The Long-Term Average Performance of Flat-Plate Solar-Energy Collectors, Sol. Energy. 7 (1963) 53–74. doi:10.1016/0038-092X(63)90006-9.